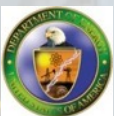# Double DVCS with CLAS12 in Hall-B

S. Stepanyan

Jefferson Lab

Towards improved hadron femtography with hard exclusive reactions 2023

Jefferson Lab, August 7 – 11

Outline

- 3D structure of the nucleon and GPD framework
- DVCS and TCS
- Extraction of GPDs from experimental observables
- Opportunities with DDVCS
- μCLAS12 for operations @ $L > 10^{37} cm^{-2} sec^{-1}$
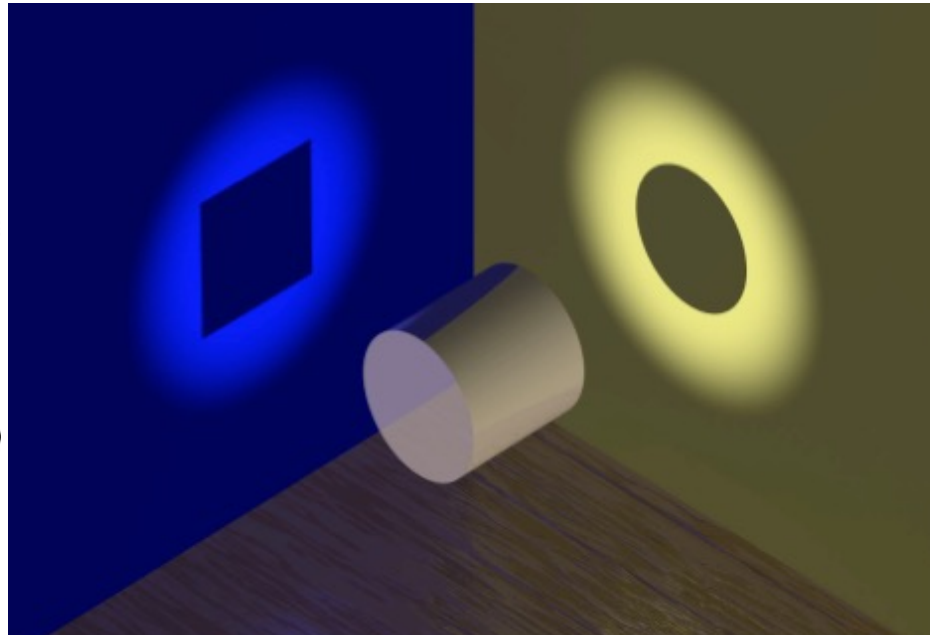 - Experimental projections
  - Reach at higher energies
- Summary

3-D Structure of the Nucleon

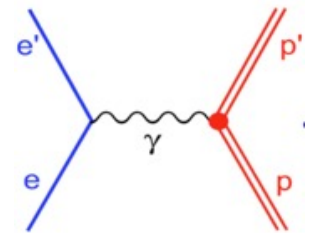Elastic and deep inelastic scatterings give us two orthogonal projections.

DIS Parton Distribution Functions
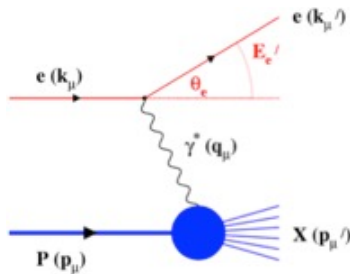
No information on the spatial location of the constituents

Elastic Form Factors

No information about the underlying dynamics of the system

Advances in theory over the past 25 years – development of formalisms of Generalized Parton Distributions – laid the path towards 3-D imaging of the nucleon's partonic structure and determination of nucleons' fundamental properties using deep exclusive.

GPD framework

- GPDs describe the correlation of quark/antiquark transverse spatial and longitudinal momentum, and the quark angular momentum distributions.
- They exhibit several interesting properties, such as *polynomiality* and subject to several constraints:

  - in the forward limit ($\xi \to 0, t \to 0$) H and $\widetilde{H}$ GPD reduce to quark, anti-quark, and gluon PDFs
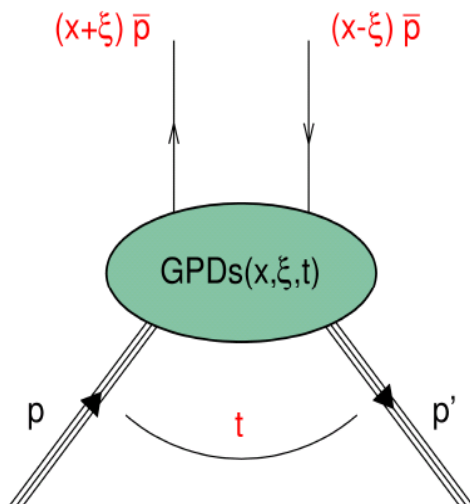
$$H^q(x,0,0) = q(x), -\bar{q}(-x)$$

$$\widetilde{H}^q(x,0,0) = \Delta q(x), \Delta \bar{q}(-x)$$

  - and the first moments of quark GPDs are related to the Dirac, Pauli, axial, and pseudoscalar form factors

$(x+\xi)\,\bar{p}$ $(x-\xi)\,\bar{p}$

GPDs(x,ξ,t)

p   t   p'

At leading-twist, there are four chiral-even (parton helicity-conserving) GPDs:

$$H^q; E^q; \widetilde{H}^q; \widetilde{E}^q$$

$$\int_{-1}^{+1} dx H^q(x,\xi,t) = F_1^q(t) \qquad \int_{-1}^{+1} dx E^q(x,\xi,t) = F_2^q(t)$$

$$\int_{-1}^{+1} dx \widetilde{H}^q(x,\xi,t) = g_A^q(t) \qquad \int_{-1}^{+1} dx \widetilde{E}^q(x,\xi,t) = h_A^q(t)$$

Nucleon EMT FF, GFF and GPDs

The QCD EMT of the nucleon:

$$\langle p', s' | \hat{T}^a_{\mu\nu}(x) | p, s \rangle = \bar{u}' \left[A^a(t) \frac{\gamma_{\{\mu} P_{\nu\}}}{2} + B^a(t) \frac{i\, P_{\{\mu} \sigma_{\nu\}\rho} \Delta^\rho}{4m} + D^a(t) \frac{\Delta_\mu \Delta_\nu - g_{\mu\nu} \Delta^2}{4m} + m\, \bar{c}^a(t)\, g_{\mu\nu} \right] u$$

The Mellin moments of GPDs linked to the EMT FF -

$$\int_{-1}^{1} dx\ x H^q(x, \xi, t) = A^q(t) + \xi^2 D^q(t)$$

$$\int_{-1}^{1} dx\ x E^q(x, \xi, t) = B^q(t) - \xi^2 D^q(t)$$

and the nucleon spin -

$$J_Q = \sum_q \frac{1}{2} \int_{-1}^{1} dx\ x (H^q(x, \xi, 0) + E^q(x, \xi, 0))$$

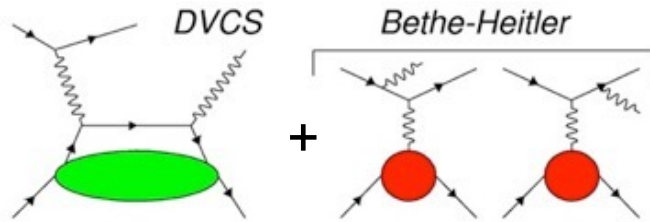Ji, Phys. Rev. Lett 77 / Phys. Rev. D 55, 1997.

And the *D*-term characterizes the distribution of forces inside the nucleon and be inferred from GPD dispersion relation.

$$\mathrm{Re}\mathcal{H}(\xi, t) = D(t) + \mathcal{P} \int_{-1}^{1} dx \left(\frac{1}{\xi - 1} - \frac{1}{\xi + 1} \right) \mathrm{Im}\mathcal{H}(\xi, t)$$

Accessing GPDs experimentally – DVCS

A large set of observables: beam helicity, longitudinal and transverse polarized target asymmetries, and cross sections.

DVCS   Bethe-Heitler

Access various combinations of CFFs

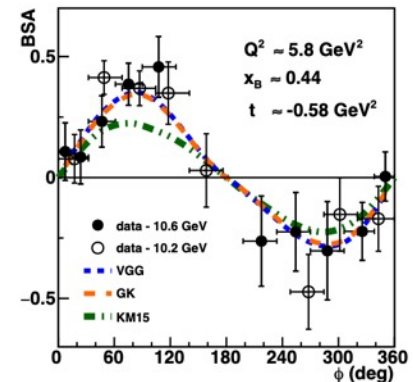$$A_{LU} \propto Im\mathcal{H}(\widetilde{\mathcal{H}}, \mathcal{E}) \qquad A_{LL} \propto Re\widetilde{\mathcal{H}}(\mathcal{H})$$
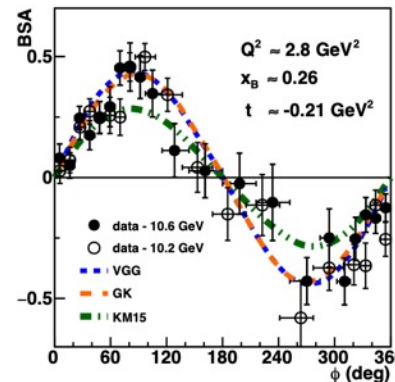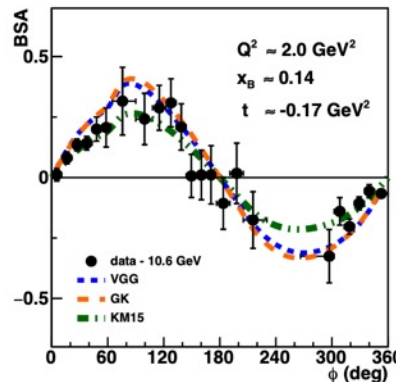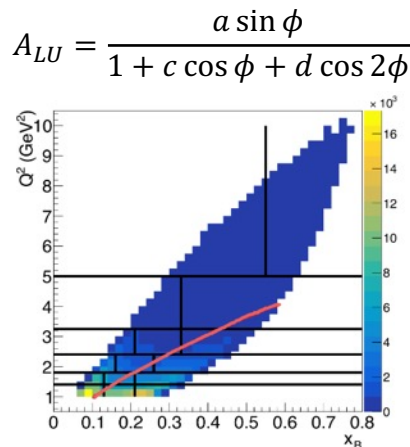
$$A_{UL} \propto Im\widetilde{\mathcal{H}}(\mathcal{H}) \qquad A_{UT} \propto Im\mathcal{E}(\mathcal{H})$$

$$ep \rightarrow e'p'\gamma = \sigma_{BH} + \sigma_{DVCS} + \sigma_{Int}$$

and a flavor decomposition, *p/n*

$$\mathcal{T}^2 = \left|\mathcal{T}_{BH}\right|^2 + \left|\mathcal{T}_{DVCS}\right|^2 + \mathcal{T}_{DVCS}^*\mathcal{T}_{BH} + \mathcal{T}_{BH}^*\mathcal{T}_{DVCS}$$

Comparisons with KM15 and VGG/GK models.

$$A_{LU} = \frac{a \sin \phi}{1 + c \cos \phi + d \cos 2\phi}$$

G. Christiaens et al. (CLAS Collaboration) Phys. Rev. Lett. 130, 211902

OFFICE OF SCIENCE

Jefferson Lab
Thomas Jefferson National Accelerator Facility

TCS with CLAS12

TCS

Bethe-Heitler (BH)

+
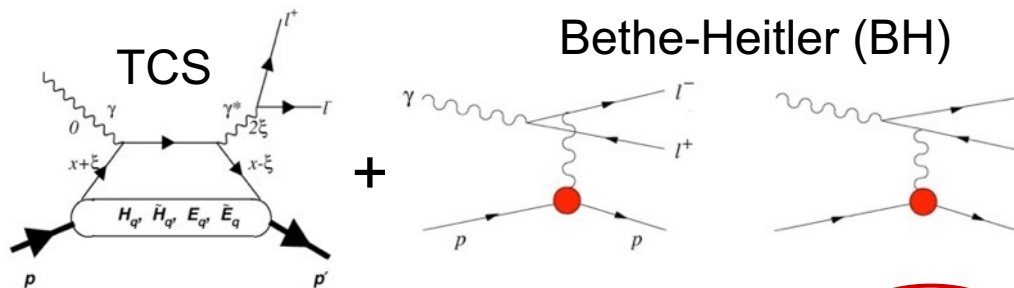
$$\sigma(\gamma\mathbf{p} \to \mathbf{p}'\mathbf{e}^+\mathbf{e}^-) = \sigma_{\mathbf{BH}} + \sigma_{\mathbf{TCS}} + \sigma_{\mathbf{INT}}$$

- BHA, $A_{\odot U} \sim \sin\varphi Im M^{--}$, universality of GPDs

- FB asymmetry, $A_{FB} \sim \cos\varphi Re M^{--}$, access to EMT FF $D^Q(t)$ (D-term).

$$A_{\odot U} = \frac{1}{P_b}\frac{N^+ - N^-}{N^+ + N^-} = \frac{d\sigma^+ - d\sigma^-}{d\sigma^+ + d\sigma^-} = \frac{-\frac{\alpha_{em}^3}{4\pi s^2}\frac{1}{-t}\frac{m_p}{Q'}\frac{1}{\tau\sqrt{1-\tau}}\frac{L_0}{L}\sin\phi\frac{(1+\cos^2\theta)}{\sin(\theta)}Im\tilde{M}^{--}}{d\sigma_{BH}}$$

$$\mathbf{A_{FB}}(\theta_0,\phi_0) = \frac{\mathbf{d}\sigma(\theta_0,\phi_0) - \mathbf{d}\sigma(\pi-\theta_0,\pi+\phi_0)}{\mathbf{d}\sigma(\theta_0,\phi_0) + \mathbf{d}\sigma(\pi-\theta_0,\pi+\phi_0)} = \frac{-\frac{\alpha_{em}^3}{4\pi s^2}\frac{1}{-t}\frac{m_p}{Q'}\frac{1}{\tau\sqrt{1-\tau}}\frac{L_0}{L}\cos\phi_0\frac{(1+\cos^2\theta_0)}{\sin(\theta_0)}Re\tilde{M}^{--}}{\mathbf{d}\sigma_{\mathbf{BH}}(\theta_0,\phi_0) + \mathbf{d}\sigma_{\mathbf{BH}}(\pi-\theta_0,\pi+\phi_0)}$$
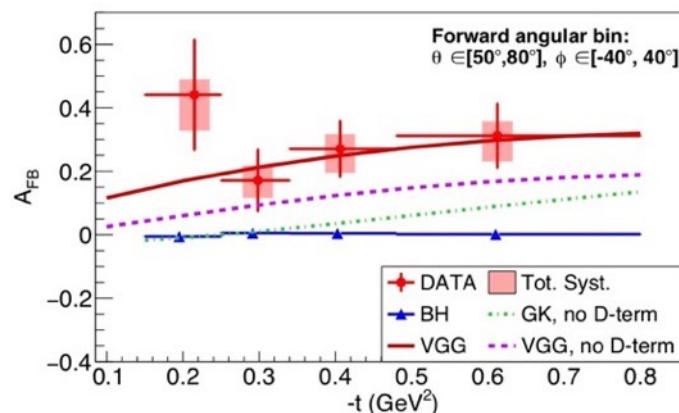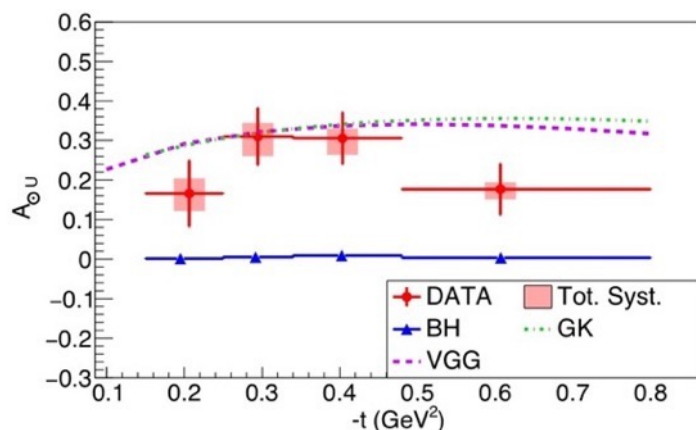
P. Chatagnon, et al. (CLAS Collaboration),"Phys. Rev. Lett. 127, 262501 (2021).

S. Stepanyan, IWHSS2022

Extracting information on GPDs

- The experimental observables (DVCS/TCS) contain complex-valued CFF.

$$\mathcal{T}_{DVCS} \sim CFF \quad \mathcal{H}(\xi,t) = \underbrace{i\pi\Big[H(\xi,\xi,t) - H(-\xi,\xi,t)\Big]}_{Im} + \underbrace{P\int_{-1}^{+1} dx\left(\frac{1}{\xi-x} \pm \frac{1}{\xi+x}\right)\Big[H(x,\xi,t) \mp H(-x,\xi,t)\Big]}_{Re}$$

- These CFFs are expressed as convolutions of complex-valued hard-scattering coefficient functions with the real-valued GPDs.

- Therefore, extracting information on GPDs from DVCS/TCS data is not straightforward and is a two-step process.

- Several extraction methods for the first step, obtaining CFFs from data at leading-twist, exist. The second step, inferring information on GPDs from CFFs, is challenging, particularly because one of the GPD variables, x, is integrated out, and the CFFs do not contain it.

- This means there can not be a unique solution going from CFF to GPDs. Various GPD functions can possibly explain experimental data at different scales.

Models of GPDs and SGPDs

- Filtering through various GPD models and parameters, will be limited by experimental uncertainties.

- Moreover, studies of deconvolution in recent years reveal existence of a class of functions, shadow GPDs (SGPD) with a null CFF and a null forward limit at a given scale μ^2, that will contribute to solutions in the GPD extraction.

- While the QCD evolution of GPDs in ξ and Q^2 can be used to exclude large class SGPDs, processes directly sensitive to the x dependence of GPDs will be required.
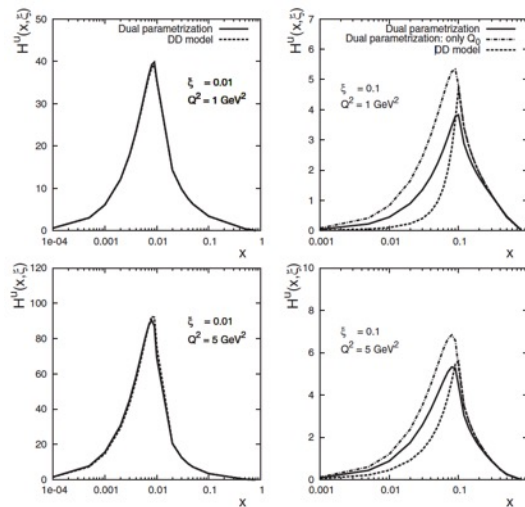
V. Guzey and T. Teckentrup, Phys. Rev. D 74, 054027 (2006)
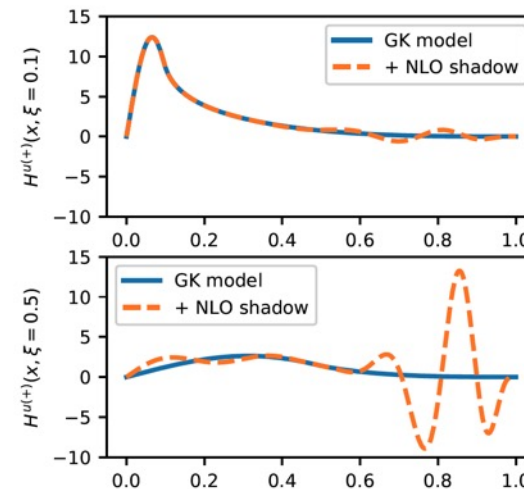
V. Bertone, H. Dutrieux, C. Mezrag, H. Moutarde, and P. Sznajder, Phys. Rev. D 103, 114019 (2021)

Closing the loop on virtual Compton scattering

First experimental measurement with CLAS12 PRL 127, 262501 (2021)

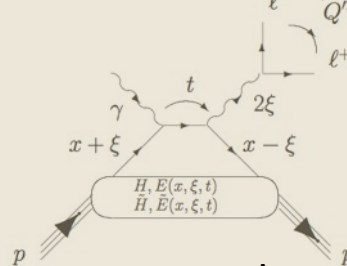**Started in 2001, PRL 87, 182002. Now is the flagship physics program**

JLAB Flagship program – accessing GPDs through measurements of beam/target asymmetries and the cross sections of Compton processes (TCS and DVCS)

TCS

Hard scale is defined by time-like photons

$$Re\,\mathcal{H}(\xi,t) = PV \int_{-1}^{1} dx\, C^{-}(\xi,x) H(x,\xi,t)$$

$$Im\,\mathcal{H}(\xi,t) = i\pi H(\xi,\xi,t)$$

Access to the Re-part of the Compton amplitude

DVCS

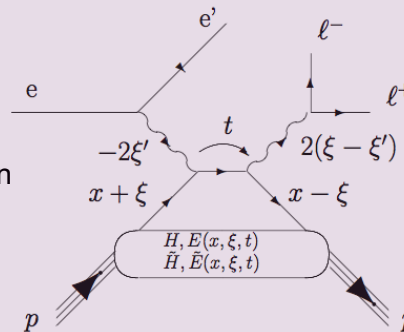Hard scale is defined by space-like photon
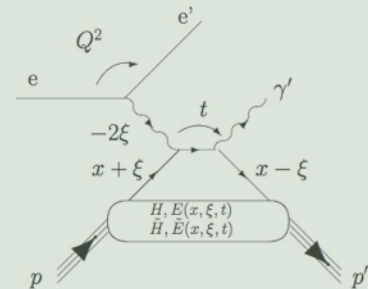
Jefferson Lab at the luminosity frontier is the only place in the world DDVCS can be measured!

μCLAS12 in Hall B and SoLID in Hall A are the two proposed facilities capable of carrying out such measurements.

DDVCS

Both space-like and time-like photons can set the hard scale

$$\int_{-1}^{+1} dx \frac{H(x,\xi,t)}{x - (2\xi' - \xi) + i\epsilon} + \dots$$

$$H(2\xi' - \xi, \xi, t) + H(-(2\xi' - \xi), \xi, t)$$

σ-DDVCS is three orders of magnitude smaller than σ-DVCS
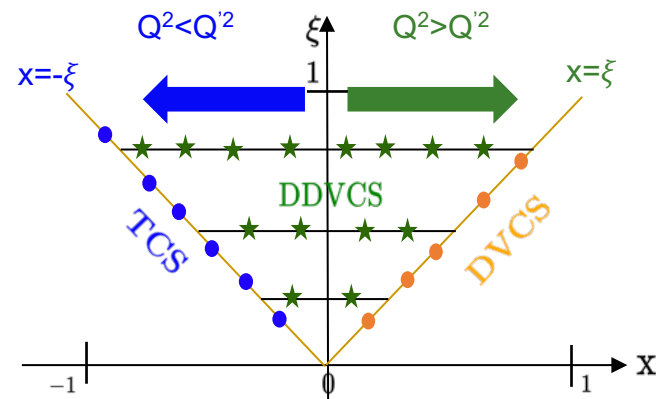
CFFs and GPDs in Virtual Compton Scattering

$$\mathcal{T}_{DVCS} \sim CFF \ \mathcal{H}(\xi,t) \propto i\pi[H(\xi,\xi,t) - H(\xi,\xi,t)] +$$
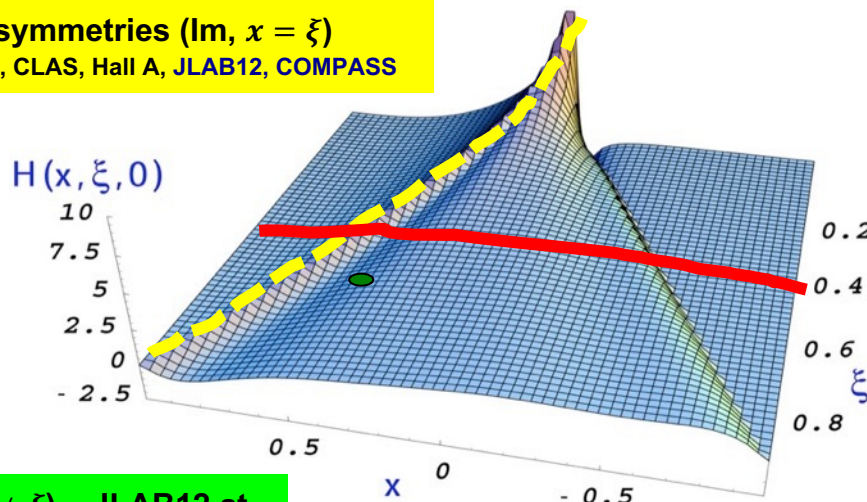$$P\int_{-1}^{+1} dx \left(\frac{1}{x-\xi} \pm \frac{1}{x+\xi}\right)[H(x,\xi,t) \mp H(x,\xi,t)]$$

(the same for TCS)

$$\mathcal{T}_{DDVCS} \sim CFF \ \mathcal{H}(\xi,\xi',t) \propto i\pi[H(2\xi'-\xi,\xi,t) - H(-2\xi'+\xi,\xi,t)] +$$
$$P\int_{-1}^{+1} dx \left(\frac{1}{x-(2\xi'-\xi)} \pm \frac{1}{x+(2\xi'-\xi)}\right)[H(x,\xi,t) \mp H(x,\xi,t)]$$

$Q^2 < Q'^2$ $Q^2 > Q'^2$

$x=-\xi$ $x=\xi$

DDVCS

TCS   DVCS

Spin asymmetries (Im, $x = \xi$)
HERMES, CLAS, Hall A, JLAB12, COMPASS

Angular asymmetry in TCS (|Re|)
JLAB12

Charge asymmetry in DVCS (|Re|)
HERMES, COMPASS, JLAB12

DVCS Cross sections (|Re|²)
H1, Hall A, JLAB12, COMPASS

$H(x,\xi,0)$

DDVCS (Im, $x \neq \xi$) – JLAB12 at
$L \geq 10^{37} \ cm^{-2} \ sec^{-1}$

Re parts of CFFs provides a direct measurement of the D-term and access to the mechanical properties of the proton

Cross section

DVCS & BH

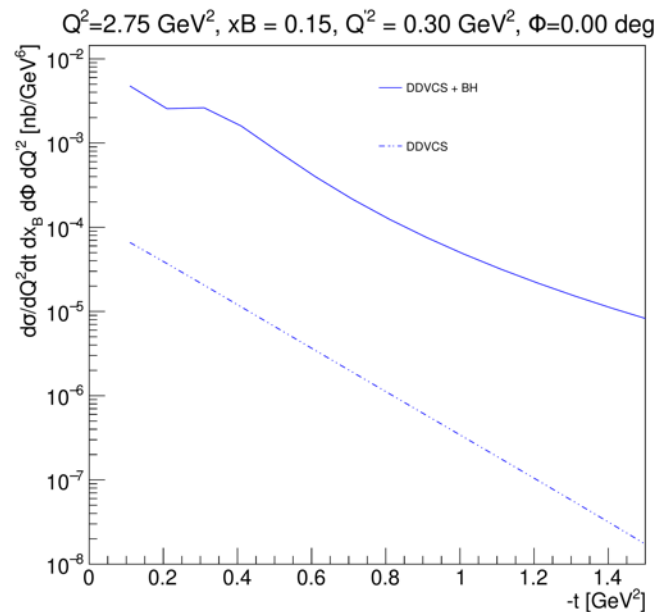$$Q^2 = -q^2 = (e - e')^2$$
$$x_B = \frac{Q^2}{2pq}$$
$$t = (p - p')^2$$

DDVCS & BH

$$Q'^2 \equiv M^2 = (l^+ - l^-)^2$$
$$\xi' = \frac{Q^2 + Q'^2}{2Q^2/x_B - Q^2 - Q'^2 + t} \xrightarrow{Q^2 \gg} \frac{x_B}{2 - x_B}$$
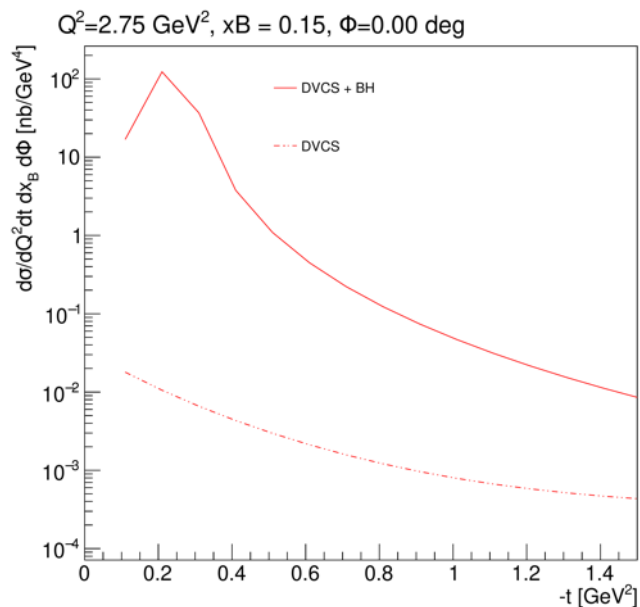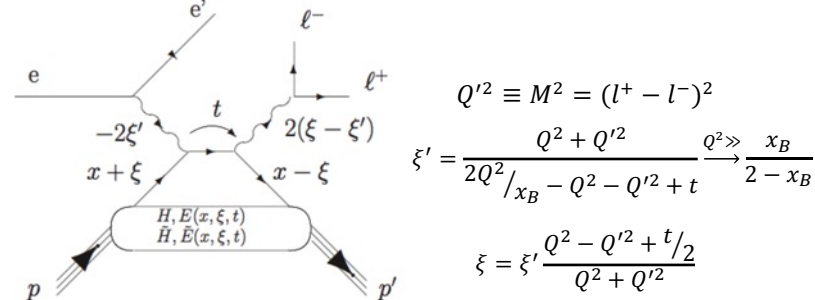$$\xi = \xi' \frac{Q^2 - Q'^2 + {}^t/_2}{Q^2 + Q'^2}$$
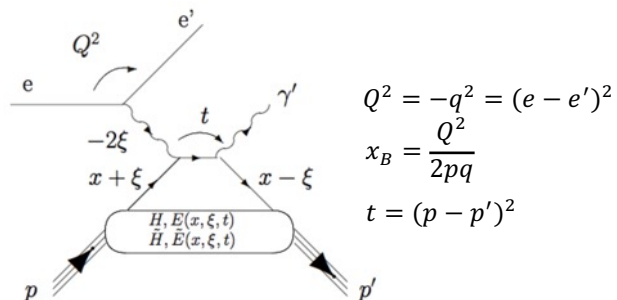
Cross sections from R. Paremuzyan, VGG code

High luminosity CLAS12 for DDVCS

Two main challenges in DDVCS measurements:

a) Cross section is three orders of magnitude smaller than the DVCS cross section;

b) Ambiguities and anti-symmetrization issues with the decay leptons of the outgoing virtual photon and the incoming-scattered lepton.

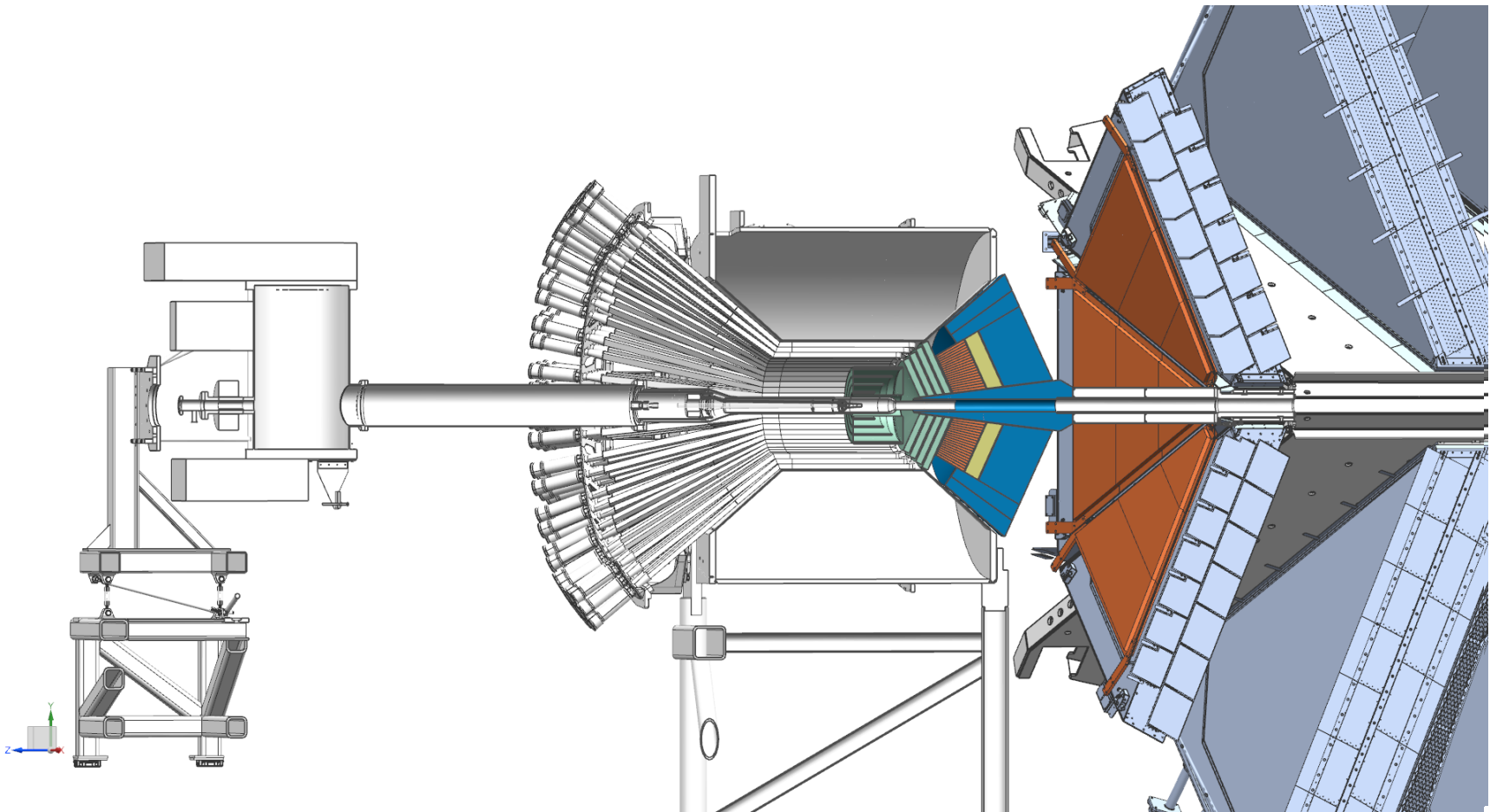Di-muon electroproduction using upgraded CLAS12 will overcome these challenges.

μCLAS12

Shield

Trackers
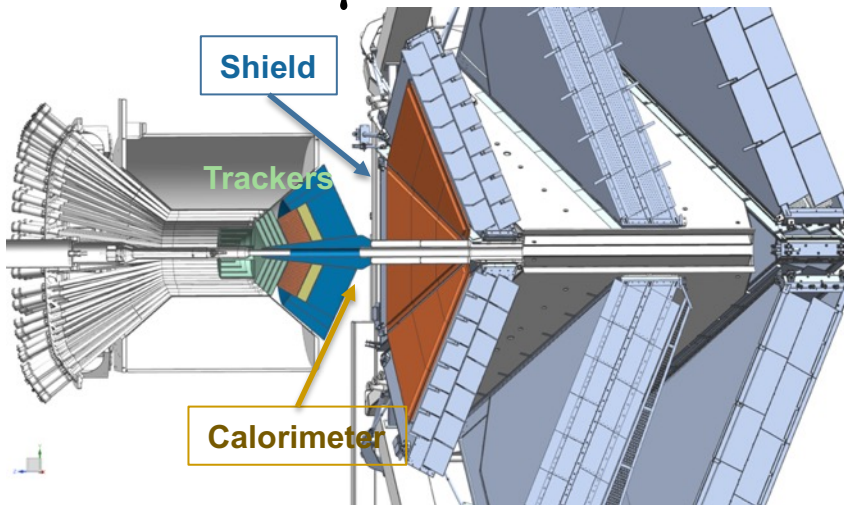
Calorimeter

A simple concept:

- Remove HTCC and block the CLAS12 forward with a W-shield and $PbWO_4$ calorimeter to prevent flooding of DC by EM background;

- Scattered electrons will be detected in the calorimeter, while shield will work as pion filter, as most of charged pions will shower and will not reach to the forward tracking system;

- Remove CVT, instead use a high rate MPGDs for central and forward (in front of the calorimeter) tracking
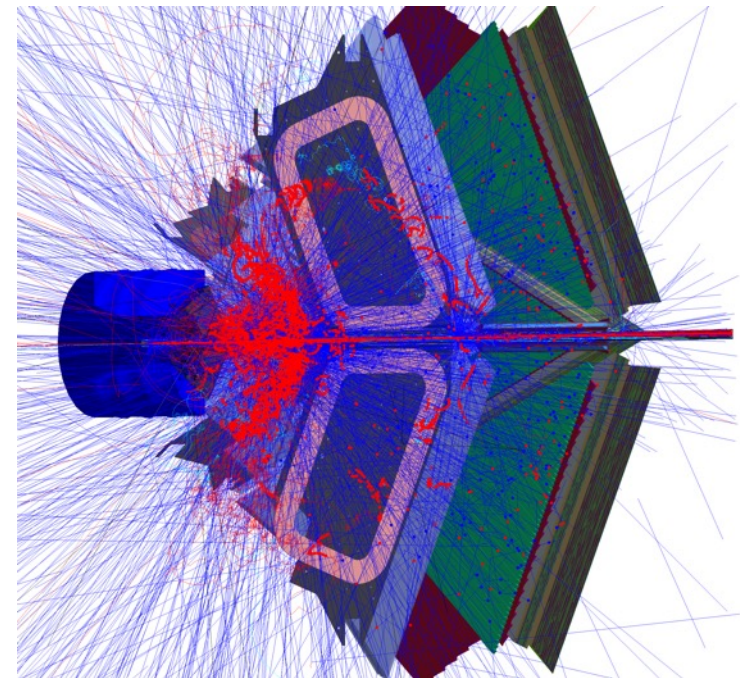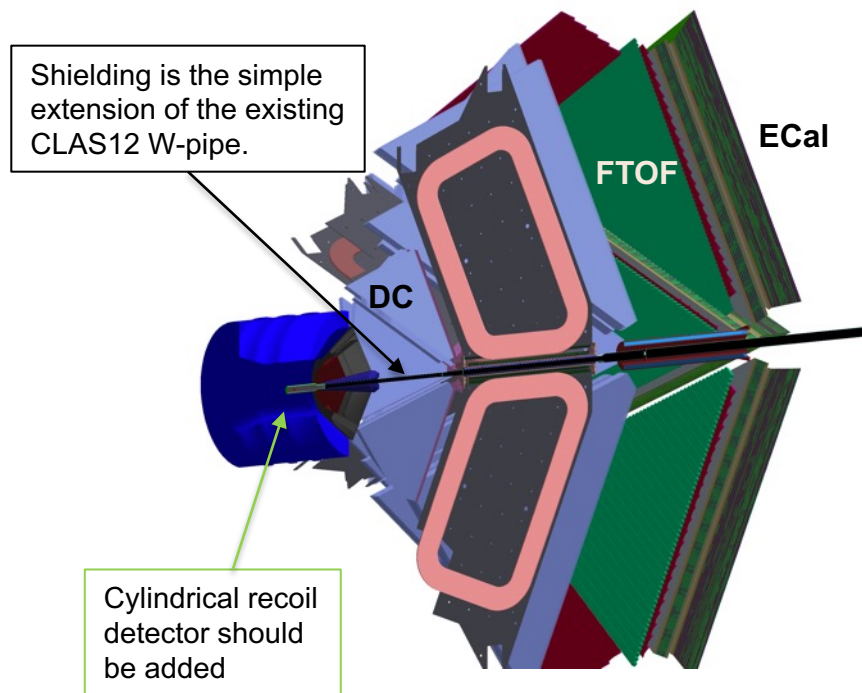
Detector capable of measuring

$$ep \rightarrow e'p'\mu^+\mu^- \ @ \ L > 10^{37}\,cm^{-2}sec^{-1}$$

Starting from CLAS12 FD with μ-RWELL
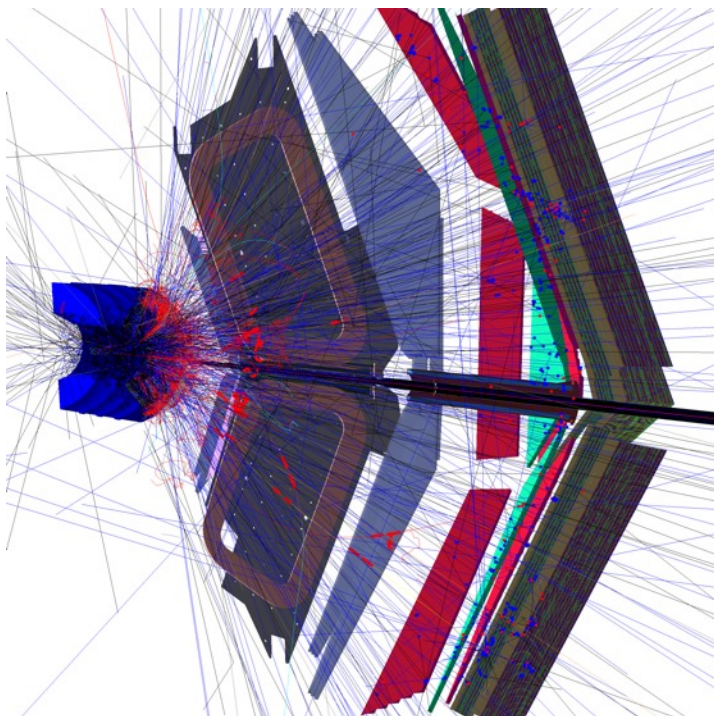# Covering CLAS12 FD12 with a μ-Spectrometer

GEANT4 model

- The forward part of the proposed upgrade (calorimeter and the shielding) is in the CLAS12 MC, GEMC (M. Ungaro).
- Simulations are underway to understand backgrounds in detectors, optimize shielding and determine luminosity limitations. (*Earlier studies for LOI12-16-004 validated the concept for* $L = 10^{37} cm^{-2} sec^{-1}$)

Shielding is the simple extension of the existing CLAS12 W-pipe.

ECal

FTOF

DC

Cylindrical recoil detector should be added

100k 11 GeV electrons in 250 ns

μ/π − separation

6 GeV π^+

6 GeV μ^+

ECal

Most pions will shower in the calorimeter/shielding and will not reach drift chambers, much less the ECal.
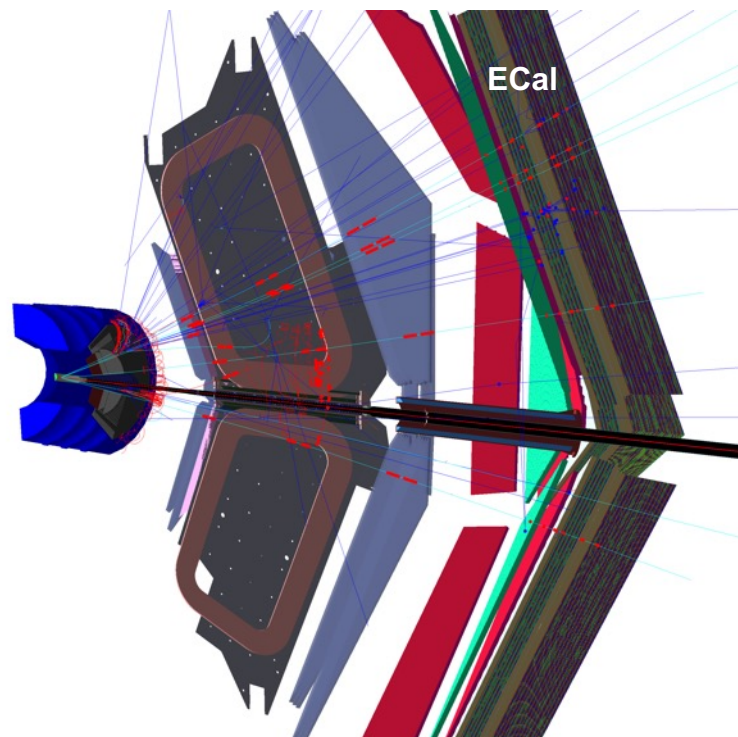
Conversely, muons will lose some energy in the calorimeter/shielding but will reach drift chambers and Ecal. Ecal is where muons are IDed.

Kinematical coverage for DDVCS

- GRAPE event generator, BH only.

- Shown one t-bin, but measurements can be extended to $-t \sim 1$ GeV^2.
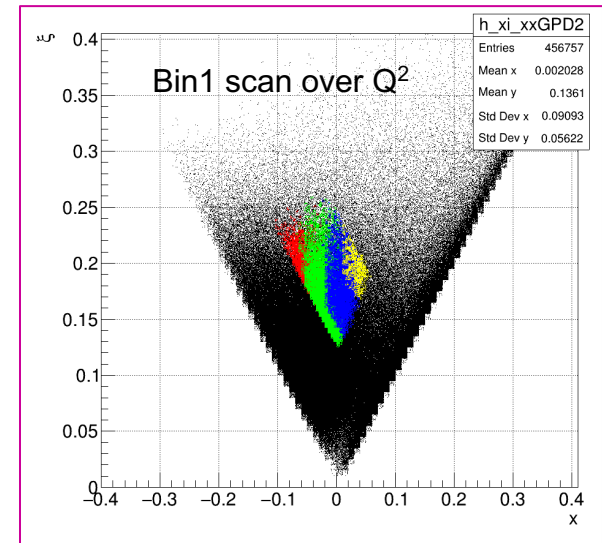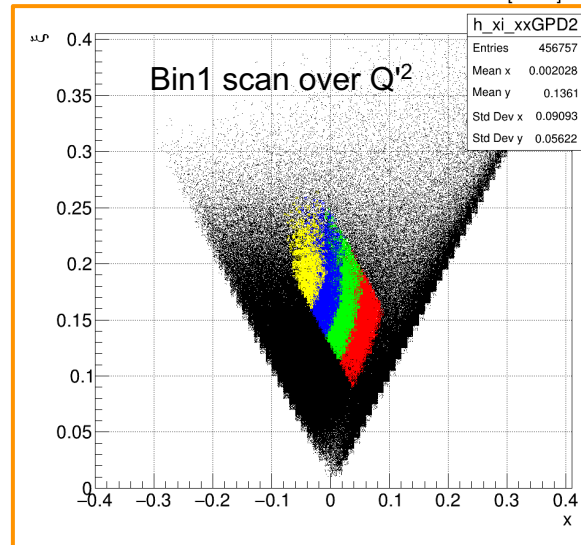
- The whole region is measured simultaneously.
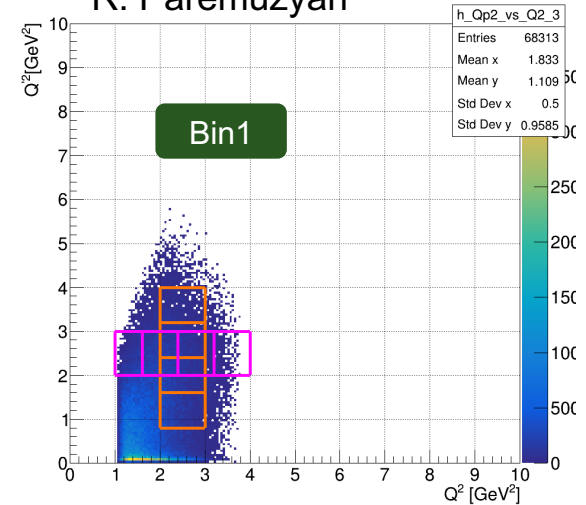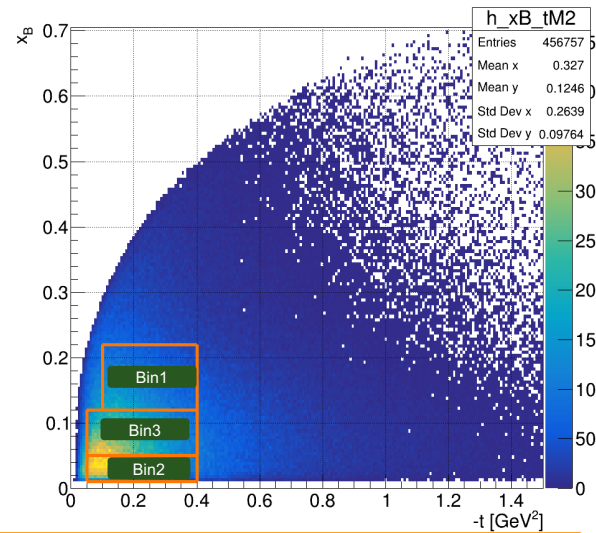
$$Q^2 = -q^2 = (e - e')^2$$

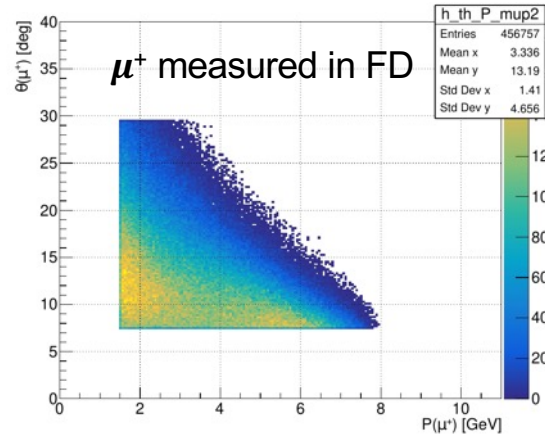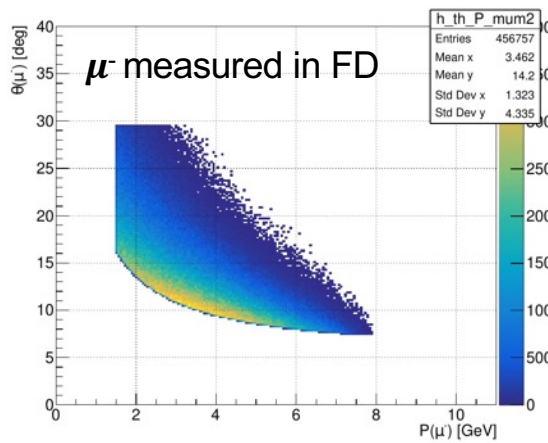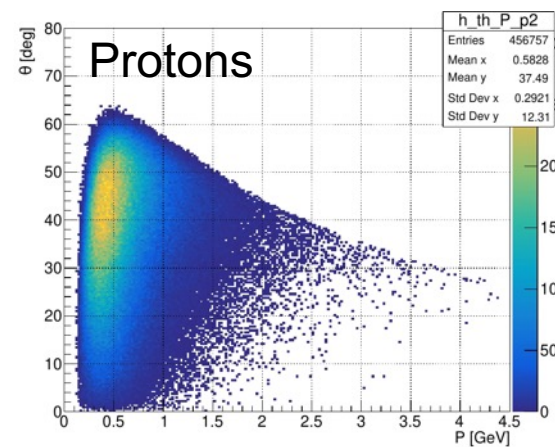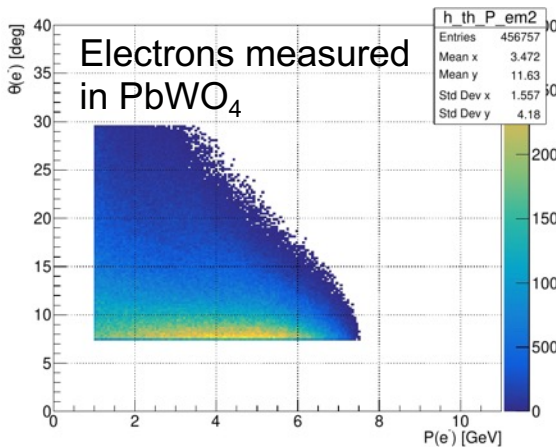$$x_B = \frac{Q^2}{2pq}$$

$$Q'^2 \equiv M^2 = (l^+ - l^-)^2$$

$$\xi' = \frac{Q^2 + Q'^2}{2Q^2/x_B - Q^2 - Q'^2 + t}$$

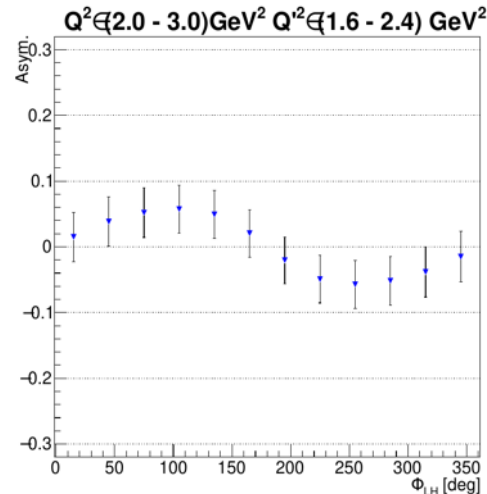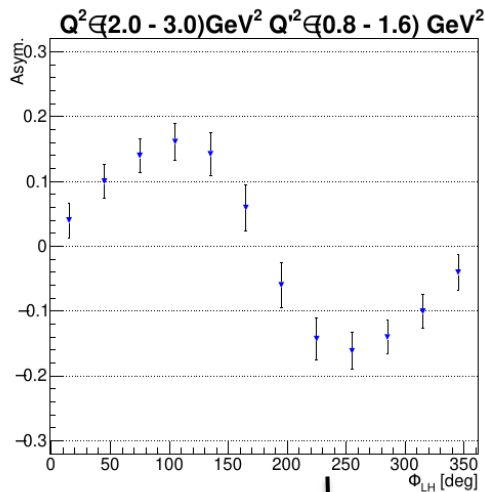$$\xi = \xi' \frac{Q^2 - Q'^2 + t/2}{Q^2 + Q'^2}$$

R. Paremuzyan

Final state particles

- Electrons and muons are confined within the calorimeter and FD.
- Recoil proton detection will be limited to $\vartheta > 40^o$, not crucial for DDVCS.
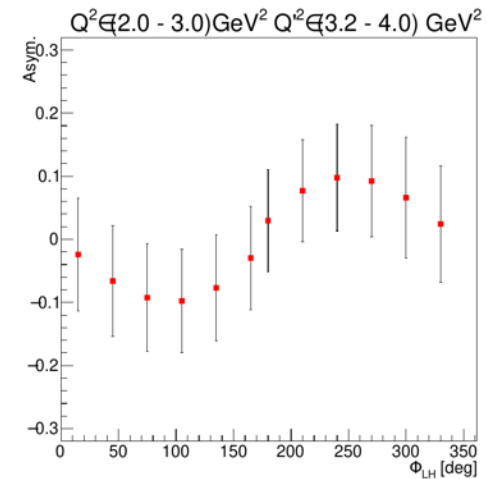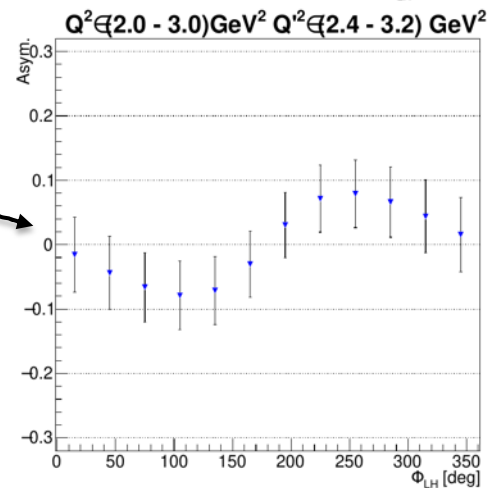
Projections for BSA: Bin1
100 days @ $10^{37} cm^{-2} sec^{-1}$

Space-like region, $Q^2 > Q'^2$

BSA sign change

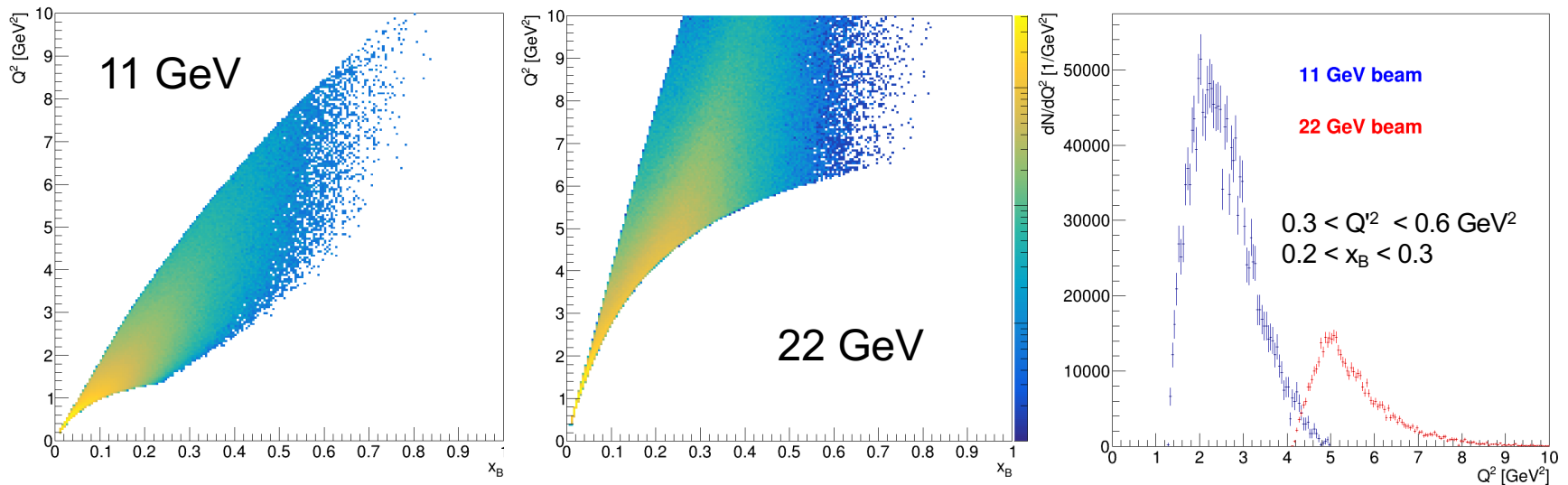Time-like region, $Q^2 < Q'^2$

How about 20+ GeV?

- CLAS12 will perform with higher energy beams, providing a significant coverage at large Q^2.
- Incremental improvements of the tracking detectors can help to retain momentum resolution for high momentum tracks.
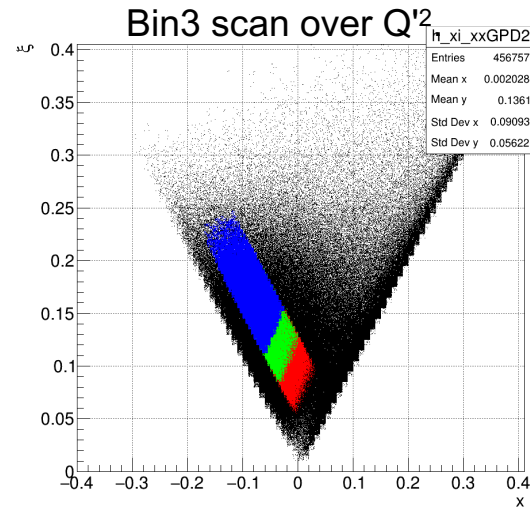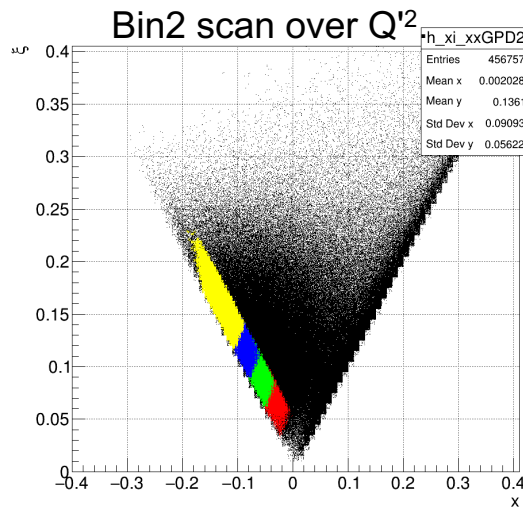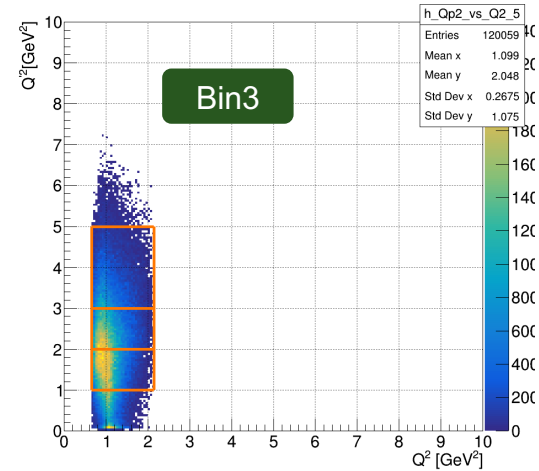- Available PID will be sufficient for exclusive and for the most of semi-inclusive reactions.
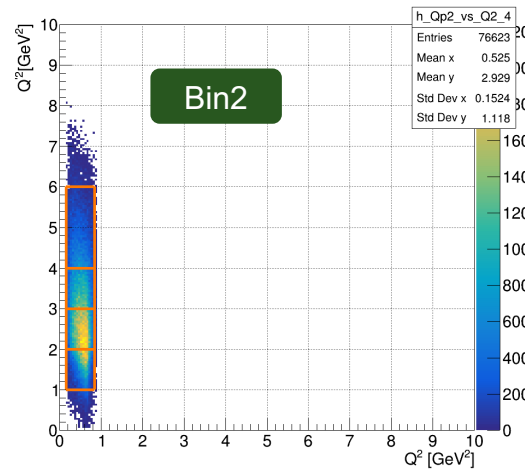
$$\mu CLAS12, ep \rightarrow e'p'\mu^+\mu^-$$

Summary

- The description of the partonic structure of hadronic matter is a major thrust of the JLab 12 GeV.

- The Compton scattering is the golden reaction for mapping GPDs, and a large set of data from DVCS and TCS measurements are already available for phenomenological analysis.

- These data (DVCS & TCS) are crucially important yet limited for inferring information on GPDs from experimental observables, as one of the GPD variables (x) is completely integrated out.

- Double DVCS, on the other hand, allows mapping of GPDs in the x-space, and Jefferson lab, home to high luminosity experiments, is the only place DDVCS can be studied.

- CLAS12 in Hall B, with modest upgrades, and SoLiD in Hall-A, can provide a wealth of data on DDVCS in a wide kinematic range.

- Also, exciting opportunities for DDVCS exist with positron beams and high energy, >20 GeV, machine.

More kinematics to explore

CLAS12 ECal for muon ID

μ+ μ- Invariant Mass

J/ψ Yield	130.9 ± 26.7
Mean	3.082 ± 0.006
σ	0.04414 ± 0.00739
1st order coef	61.74 ± 9.44
2nd order coef	−275 ± 64.0
3rd order coef	424.3 ± 195.9
offset	6.414 ± 2.563

Invariant Mass [GeV]
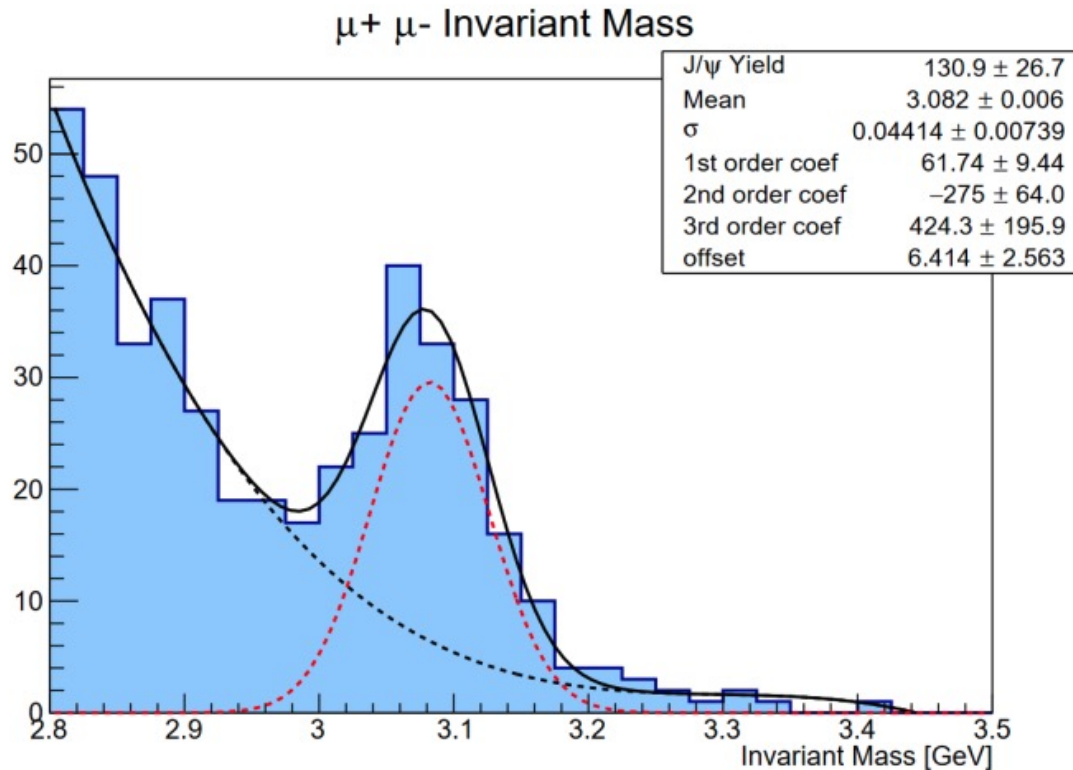
More with higher energy: XYZ spectroscopy

- Several states in charmonium region have been discovered that do not fit into a simple $q\bar{q}$ model.

- JLAB energy upgrade (20+ GeV) will open a phase space for photoproduction of some of these states.

- $\boldsymbol{\mu}$CLAS12 at 10^{37} cm^{-2} sec^{-1} will contribute in the studies of the lowest mass states.

- An example, well know exotic $\chi_{c1}(3872)$, aka X(3872), first discovered by Belle in 2003.

$$\gamma p \rightarrow \chi_{c1}(3872)p'$$
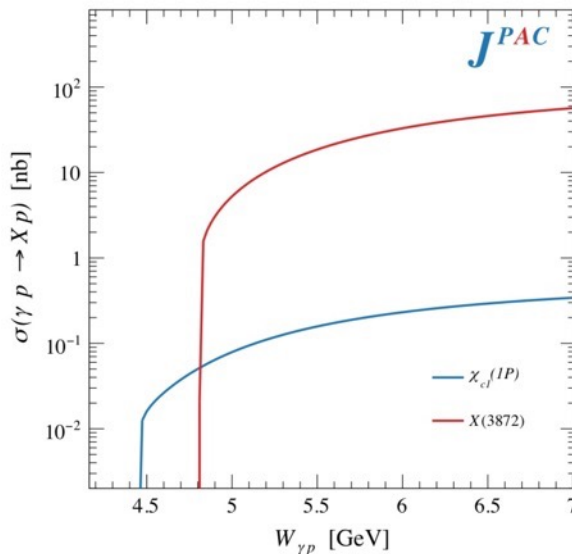
The luminosity in the energy range: 13 GeV to 22 GeV is 100 nb^{-1}, even with modest efficiency of 2% one expects **>50 detected $\boldsymbol{\chi_{c1}}$(3872) per hour** in each decay mode

$\chi_{c1}(3872)$ decay modes:

- $\chi_{c1} \rightarrow \omega J/\psi$ BR= 4.3%
  $\omega \rightarrow \gamma\pi^0$ BR=8.28%
  $J/\psi \rightarrow \mu^+\mu^-$ BR=6%
  $\chi_{c1} \rightarrow \gamma\gamma\gamma\mu^+\mu^-$ BR≥ 2x10^{-4}

- $\chi_{c1} \rightarrow \gamma\,\psi(2S)$ BR= 4%
  $\psi(2S) \rightarrow \mu^+\mu^-$ BR=0.8%
  $\chi_{c1} \rightarrow \gamma\mu^+\mu^-$ BR≥ 2.3x10^{-4}

Nucleon EMT FF, GFF and tomography

$$\langle p', s'|\hat{T}^a_{\mu\nu}(x)|p, s\rangle = \bar{u}'\left[A^a(t)\frac{\gamma_{\{\mu}P_{\nu\}}}{2} + B^a(t)\frac{i\,P_{\{\mu}\sigma_{\nu\}\rho}\Delta^\rho}{4m} + D^a(t)\frac{\Delta_\mu\Delta_\nu - g_{\mu\nu}\Delta^2}{4m} + m\,\bar{c}^a(t)\,g_{\mu\nu}\right]u$$
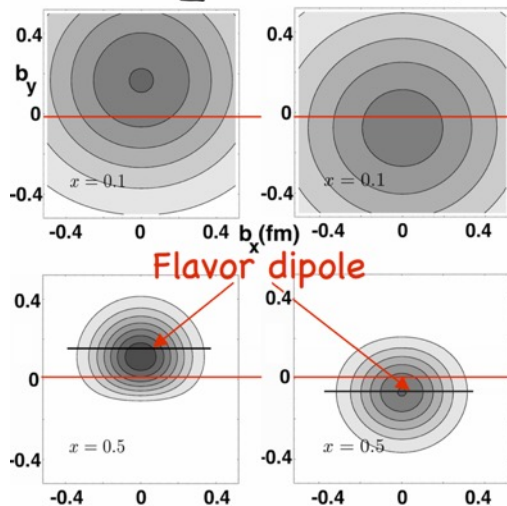
Link to the energy-momentum tensor

$$\int_{-1}^{1} dx\; xH^q(x, \xi, t) = A^q(t) + \xi^2 D^q(t)$$

$$\int_{-1}^{1} dx\; xE^q(x, \xi, t) = B^q(t) - \xi^2 D^q(t)$$

$$H^q(x, b_\perp) = \int \frac{d^2\Delta_\perp}{(2\pi)^2} e^{-ib_\perp\Delta_\perp} H^q(x, 0, -\Delta_\perp^2)$$

Decomposition of the nucleon spin

$$J_Q = \sum_q \frac{1}{2} \int_{-1}^{1} dx\; x(H^q(x, \xi, 0) + E^q(x, \xi, 0))$$

$u_x(x, b_\perp)$ $d_x(x, b_\perp)$

Flavor dipole

M. Burkardt, Int.J.Mod.Phys.A18,2003

Nucleon tomography

Ji, Phys. Rev. Lett 77 / Phys. Rev. D 55, 1997.

$$\text{Re}\mathcal{H}(\xi, t) = D(t) + \mathcal{P}\int_{-1}^{1} dx\left(\frac{1}{\xi - 1} - \frac{1}{\xi + 1}\right)\text{Im}\mathcal{H}(\xi, t)$$

the *D*-term characterizes the distribution of forces inside the nucleon

Polyakov, Physics Letters B 555, 2003